POLYLACTIDE-BASED COMPOSITE MATERIALS FOR 3D PRINTING AND MEDICAL APPLICATIONS - THE EFFECT OF BASALT AND SILICON DIOXIDE ADDITION

Maciej Pyza[1]*, Natalia Brzezińska[1], Karolina Kulińska[2], Jadwiga Gabor[1], Adrian Barylski[1], Krzysztof Aniołek[1], Żaneta Garczyk-Mundała[1], Kayode Adebesin[1], Andrzej Swinarew[1,2]

[1] Faculty of Science and Technology, University of Silesia, 75 Pułku Piechoty 1A, 41-500 Chorzów, Poland
[2] Institute of Sport Science, The Jerzy Kukuczka Academy of Physical Education, Mikołowska 72A, 40-065 Katowice, Poland
*e-mail: maciej-pyza@wp.pl

Abstract

Polymers are compounds that play a key role in the development of many fields of science, including emergency medicine. Currently, there are increasing requirements for biomedical polymers in terms of producing lighter and more ecological equipment. To meet these requirements, a composite material was developed: polylactide (PLA) with the addition of modifiers - basalt and silicon dioxide (SiO_2). PLA was chosen as a biodegradable polymer that naturally decomposes in the environment. This is very important, regarding a large number of single-use materials made of microplastics polluting the environment. The samples were made by additive 3D printing and then immersed in swimming pool water, chlorine solution, and distilled water. FTIR analysis showed the influence of the environment on the intensity and shift of PLA absorption bands. Microscopic analysis provided information on surface morphology, roughness, and potential defects. Tribological and micromechanical tests showed that the additions of basalt and silica to the PLA material influenced the morphological structure and the average area of the wear trace, volumetric wear, and average coefficient of friction. In the presence of chlorine solution, distilled water, and pool water under real conditions, the SiO_2 addition made the PLA material more resistant to abrasion, as compared to the basalt addition. However, additives did not significantly affect the PLA material hardness, and the samples with basalt turned out to be more resistant to deformation.

Keywords: *polylactide, 3D printing, polymer, basalt, SiO_2*

Introduction

Polymers are a group of compounds that are being increasingly applied in many fields. In medicine, polymers are used to produce medical devices for reconstructive surgery, cardiac surgery, transplantology, or dentistry. In addition, polymers are also successfully employed in emergency medicine and water rescue. The polymer design offers better, more ergonomic, lighter, and eco-friendlier equipment necessary to save human lives. However, the materials developed for this solution must have suitable mechanical properties as compared to traditional materials. Applications of polymers contribute to the medical market as well as to the field of additive technologies [1]. One of such materials is polylactide (PLA), i.e. an aliphatic linear polyester made of α-hydroxy acids (FIG. 1).

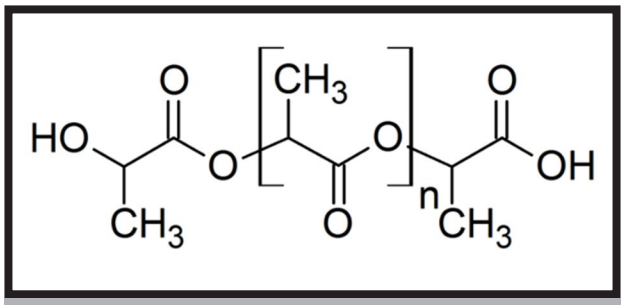

FIG. 1. PLA structural scheme.

PLA is a biodegradable, thermoplastic polyester formed in the process of polymerization of lactic acid. It is obtained as a result of the fermentation of sugars from carbohydrate sources, such as corn or sugar cane [2]. It can be produced with a capacity of more than 140,000 tons per year on a global scale, making it easily available and relatively cheap. It is one of the most promising biopolymers due to the low greenhouse gases emission and the small amount of energy used for its production [3]. PLA belongs to polyesters which are the most versatile biodegradable materials due to the presence of bonds susceptible to attack by hydrolytic enzymes in their main chain [4]. In the pharmaceutical industry, PLA is used as a carrier of active substances, and in medicine for the regeneration of damaged tissues. PLA is also increasingly found in areas such as textiles and the packaging industry. The wide variety of applications results from its good mechanical properties, i.e. tensile strength, Young's modulus, and flexural strength. Additionally, the beneficial physical and chemical properties of PLA, as well as its biocompatibility, make it applicable for drug delivery systems, medicinal products, surgical implants, orthopaedic devices, and bioresorbable scaffolds for tissue engineering [5]. However, PLA has low rate of crystallization, low strength and heat resistance that are limiting factors for its long-term use.

Additives such as mineral fibers or natural organic compounds make it possible to modify the PLA properties, including mechanical strength, chemical resistance, or plasticity. For instance, basalt fibers are 100% natural and thus environmentally friendly. They are made of igneous rocks and are non-toxic. They have high temperature resistance, chemical resistance, and mechanical properties, such as abrasion resistance [6]. Basalt is characterized by high hardness, corrosion resistance, as well as high thermal and chemical stability [7]. Such additives in the PLA material can increase its applications in various fields due to improved properties.

[Engineering of Biomaterials 166 (2022) 29-39]

doi:10.34821/eng.biomat.166.2022.29-39

Submitted: 2023-01-25, Accepted: 2023-02-22, Published: 2023-02-28

Taking into account the properties of the selected polymer matrix and its modifiers, such as SiO_2 and basalt, the plan was to obtain the material for printing by extrusion in the appropriate temperature regime. The research aimed to evaluate the properties of PLA enhanced with silica and basalt and to determine its potential applications. The samples were immersed in chlorine solution, swimming pool water, and distilled water to examine the material applicability in water and medical rescue. For this purpose, the FTIR analysis was carried out to identify changes in the chemical structure of the modified material, and the tribological analysis to assess their impact on the material wear resistance. Micromechanical testing determined the effect of additives on the micromechanical properties of the material, i.e., hardness, fracture toughness and elasticity modulus. The confocal microscopy examination visualized the material structure, its surface properties and the morphological structure changes.

The use of PLA/basalt, PLA/SiO_2 composites and the 3D printing technology provided an opportunity to develop an innovative project - an ultra-light and universal rescue board for use in water and medical rescue. Its characteristic feature is the profiled bottom distinguished by the presence of fins based on the utility model no. 67456 [8]. Such a design increases the buoyancy of the equipment and improves its efficiency in water rescue. One variant of the device assumed a "honeycomb"-type HDPE filling in the ratio of 20% full to 80% empty volume. In the research, it was decided to replace the material with the modified PLA to reduce the total weight of the device without a significant loss of strength.

Materials and Methods

In order to obtain PLA/basalt and PLA/SiO_2 composite materials, the fibers were shortened via pulverization. Each fiber of 9 g in weight was placed in the sample chamber of the Pulverizer. The rotation speed was set to 350, the repetition 47 with the timer set to 15 min for each repetition. Mixing was performed with a self-made mixer in order to homogenize the matrix and the reinforcement. For adhesive purposes, polyol was used as a homogenizing agent. The composites were vacuum dried at 55°C, under a pressure of 760 mmHg for 6 h. The extrusion took place in the temperature regime with the set appropriate parameters. The temperature parameters for the PLA/SiO_2 composite were 230°, 220°, 212° and 199°, respectively. For the PLA/basalt composite, they were 235°, 225°, 215° and 204° for the single-screw extruder with L/d = 32/1. Basalt is a volcanic material with ceramic properties. As a modifier, it enhances mechanical strength, wear resistance, and thermal stability in the 3D printed objects. On the other hand, SiO_2 is a well-known ceramic material with high hardness and wear resistance. Its presence in the composite improves the mechanical and thermal properties of the 3D printed models. PLA in the form of granules and modifiers were liquefied in a continuous process. Thanks to the use of a linear head and the synchronization of the pick-up tape, a filament with a diameter of 1.75 mm was obtained.

The first step of the 3D printing process was the preparation of spatial models using CAD software - SolidWorks. Then, thanks to the Slic3r program, they were converted into a "g-code" file, ready for use on a 3D printer. The Urbicum DX device with a working area of 305 (X) x 305 (Y) x 380 mm (Z) was employed. The set temperature parameters were 80°C for the worktable and 200-210°C for the head. For proper printing and better adhesion to the build plate, the temperatures were increased for PLA/SiO_2 and PLA/basalt by about 20°C, as compared to the pure PLA. The printing speed in the additive technology was set at 60 mm/s for the 4 inner layers and 50 mm/s for the two top layers and the two bottom layers. The average layer thickness was 0.2-0.3 mm. The "solid" type filling was used, i.e. 100%. There was no need for supports for the models. The resulting 3D printed samples were cuboid with the dimensions 50 x 50 x 10 mm (FIG. 2).

The preliminary research stage was the samples immersion in distilled water, swimming pool water, and a solution of sodium dichloroisocyanurate in distilled water (FIG. 3) for 7 days. The dissolutions ratio was 5 mg Cl_2 (1 tablet 8.5 mg of sodium dichloroisocyanurate containing 5 mg Cl_2) / 1 l H_2O (chlorine solution). The samples were drilled with a bench drill to a diameter of between 2 and 10 mm and threaded. The reference sample was the PLA material immersed in the same substances and with the same parameters as the samples containing PLA/basalt and PLA/SiO_2.

The next step was drying carried out using the DZ-3BC dryer with a power of 2000 W. It was conducted at 50°C for two hours under vacuum conditions.

The FTIR (Fourier Transform Infrared Spectroscopy) spectroscopy was carried out to evaluate the chemical composition and the molecular structure of the obtained samples. The tests were performed on the FTIR spectrophotometer - IRTracer-100, equipped with the ATR accessory (attenuated total reflectance). The measurements were made at 100 scans per sample.

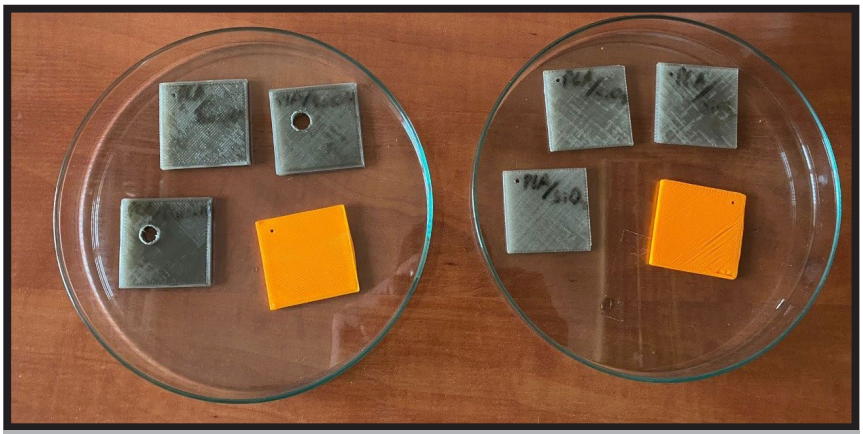

FIG. 2. Prepared test samples.

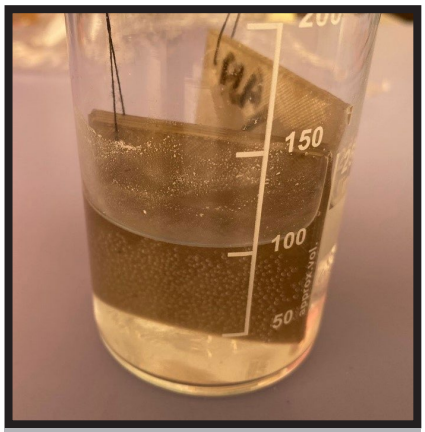

FIG. 3. An example of immersing a sample in a chlorine solution.

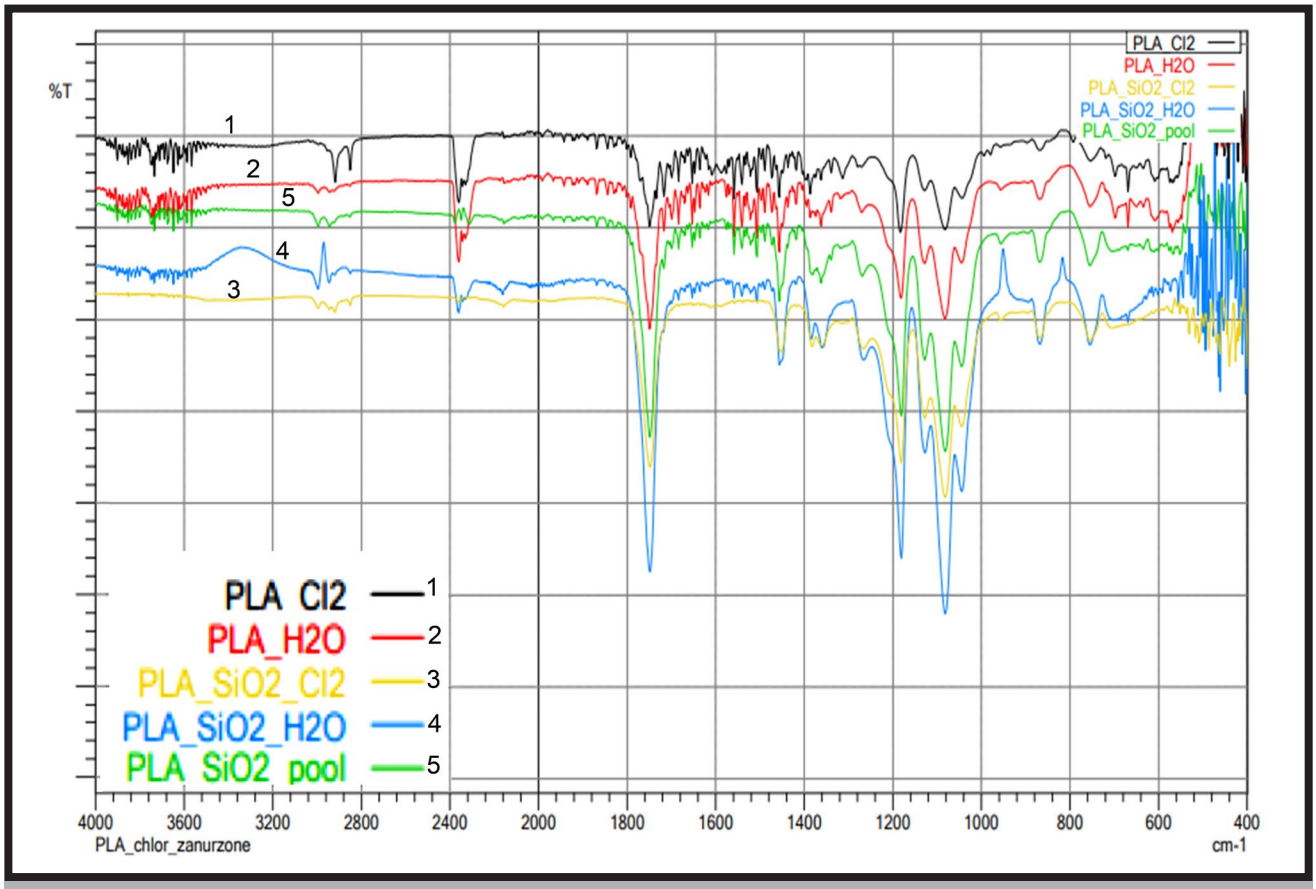

FIG. 4. Spectrum obtained for the PLA/SiO_2 sample immersed in chlorine solution, H_2O and pool water in relation to the PLA reference sample immersed in chlorine solution and H_2O.

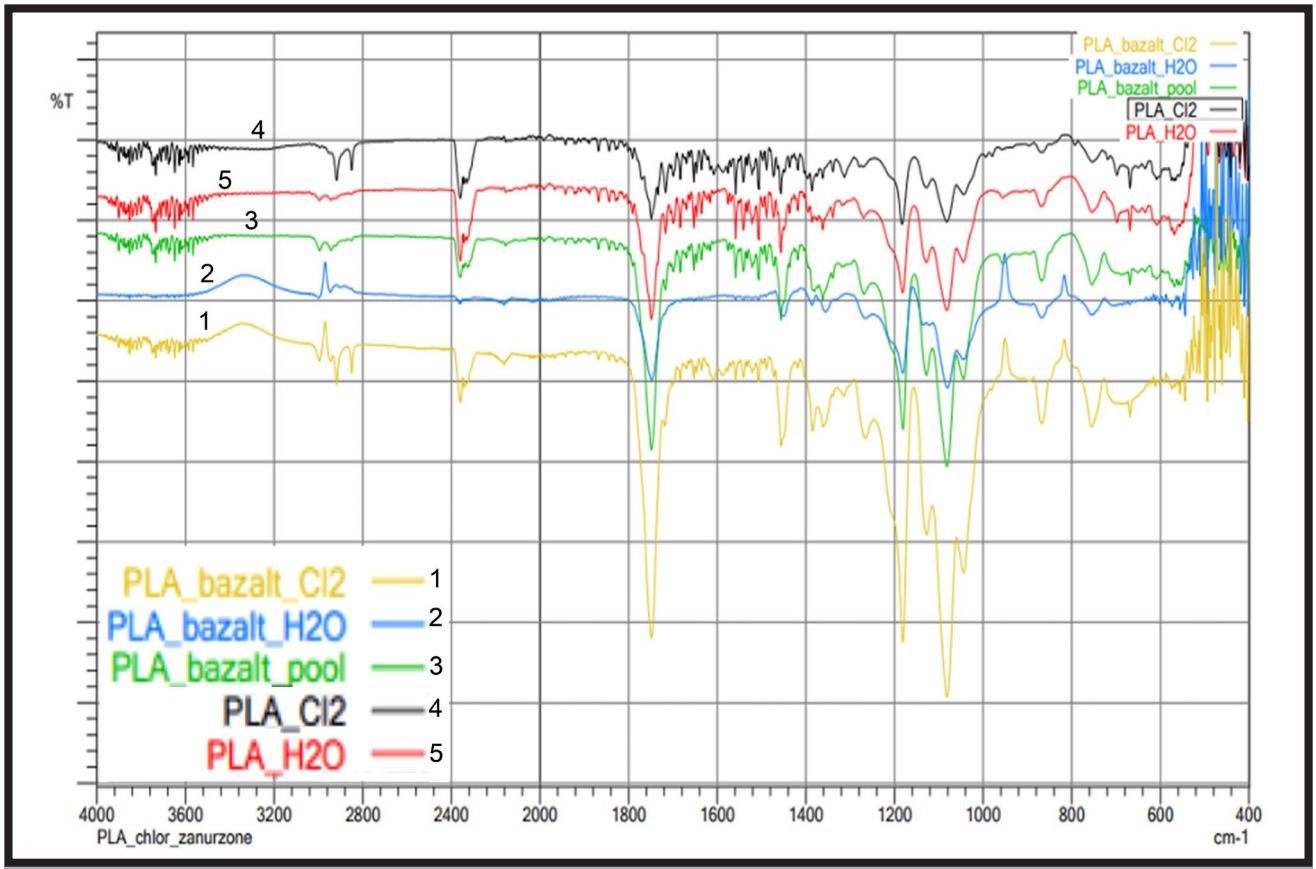

FIG. 5. Spectrum obtained for the PLA/basalt sample immersed in chlorine solution, H_2O and pool water in relation to the PLA reference sample immersed in chlorine solution and H_2O.

The LEXT OLS4000 scanning confocal microscope was used to obtain microscopic images. The surface images were analyzed using the MountainsMap® Premium software.

The material evaluation in terms of friction, wear resistance, and friction coefficient was performed via tribological tests. The dimensions of the samples were adjusted to 25 x 25 x 1 mm and then ground to remove the excess material. This was achieved by dry grounding edges with silicon carbide sandpaper with grits of P820 and P600. Tribological tests were performed using the ball-on-disc friction junction on the Anton-Paar device (Tribometer - TRN, Corcelles-Cormondrèche, Switzerland). Steel bearing balls (100Cr6) with a diameter of 6 mm were used as counter samples. The tests were carried out in conditions of the technically dry friction in a reciprocating linear motion. The pressure force in the friction node was F_N = 20 N, the friction distance amplitude L = 10 mm, the frequency f = 3.18 Hz, and the number of cycles 1250 (friction distance s = 25 m). The average wear trace area P was determined using the Surftest SJ-500 profilographometer (Mitutoyo, Tokyo, Japan). The volumetric wear Vw was determined according to the formula:

$$V_W = \frac{V}{F_N \cdot s} \left[\frac{mm^3}{Nm} \right]$$

where: F_N – load [N], s – friction distance [m], V – volume of the wear trace calculated for linear reciprocating motion from the formula $V = P \cdot L$ [mm^3], P – average wear trace area [mm^2], L – friction distance amplitude [mm] [9,10]

Micromechanical tests were performed with the Micro Combi Tester - MCT3 device (Anton Paar, Corcelles-Cormondrèche, Switzerland). The Berkovich diamond indenter (B-V 83) was used, with a maximum load of 100 mN (0.1 N). The load-unload of the indenter was performed at a speed of 200 mN/min, the holding time under a maximum load was 10 s. For each sample, 5 indentations were made. The hardness HIT and elasticity modulus EIT were determined using the Oliver-Pharr method [11]. The measurements stayed in accordance with the ISO 14577 standard [12]. On the basis of the recorded load-unload curves, the values of the total indentation work W_{tot} and its components (plastic indentation work W_{pl} and elastic indentation work W_{el}) were determined. The percentage of elastic recovery work η_{IT} was also established.

Results and Discussions

According to preliminary studies, the composite material, i.e. PLA with the addition of basalt and silica, underwent a plastic deformation due to a force causing its flow through the matrix. This material adopted the cross-sectional profile of the matrix. Thanks to the appropriate properties, the fiber shape was retained in the final phase of extrusion.

The FTIR infrared spectroscopy was carried out to determine the chemical composition of the tested samples. The examination of the characteristic bands for functional groups allowed the identification of the chemical components of the material and the changes in its chemical structure. In general, these changes are caused by the immersion in water-based environments, which may affect mechanical properties. After placing the properly prepared samples in the FTIR equipment, the following results were obtained and compared to evaluate possible differences (FIGs 4 and 5).

In the FTIR analysis of the samples, the characteristic two bands are: the absorption one of the hydroxyl group (-OH) around 3600-3200 cm^{-1}, present in the lactic acid, and the band of the aromatic group around 1600-3200 cm^{-1}. The absorption bands present in the PLA sample are the methyl group (-CH_3) 3000-2800 cm^{-1}, the carbonyl group (C=O) 1750-1700 cm^{-1}, the methylene group (-CH_2-) 1450-1350 cm^{-1}, group C-O 1300-1200 cm^{-1} and C-O-C 1150-1050 cm^{-1}. Each absorption band in the FTIR spectrum corresponds to the absorption of energy by a specific functional group, which allows to identify its presence and amount in the material [13]. Analyzing the above graphs, in the plain PLA (PLA_Cl_2, PLA_H_2O) a characteristic absorption band associated with ester carbonyl groups and CH_3 groups can be observed. Banding is typical and it appears as narrow peaks. There is also a characteristic band shift in the case of PLA_H_2O, which may be due to the water moisture.

Basalt and SiO_2 modifiers affected the characteristic absorption bands exhibited by PLA for carbonyl ester groups and methyl groups. The basalt presence made the bands shift slightly, while the addition of SiO_2 affected their intensity and shape. The characteristic absorption bands for silica are in the range of 1050-1200 cm^{-1} and the absorption bands for Si-O-Si groups are in the range of 1000-1200 cm^{-1}, while for basalt and minerals contained in it - silica and oxides are in the range of 1050-1200 cm^{-1} and 400-900 cm^{-1}, respectively [14,15].

The shape, intensity, and shift can be influenced by the samples immersion in water, chlorine solution, or pool water. Water affects the PLA chemical structure through hydrolysis of ester bonds, which leads to the polymer decomposition, and thus to its strength decrease [16]. The same applies to Cl_2 which can react with the PLA functional groups. This reaction also leads to changes in the absorption bands characteristic for these groups, via hydrolysis and the reaction with chlorine compounds [17]. Pool water has a similar effect due to chlorine. Changes in these bands indicate the chemical structure alterations and thus the changes in mechanical properties. In the analyzed samples, the absorption bands did not undergo significant shifts, nor did their shape and intensity change. However, this may change in a long-term study, hence, it needs further tests.

The examination using the LEXT OLS4000 confocal microscope produced the 3D images of the sample structures to determine the surface morphology, roughness, and potential defects that may occur in the printed samples. Their surface structure was also compared depending on the basalt/SiO_2 modifier present in the PLA material and after immersing the samples in solutions. The images were taken at different magnifications for a more detailed analysis (20x, 50x).

FIGs 6a and 7a show the microscopic images of the PLA material - a reference sample soaked in H_2O. This material has noticeable characteristics that can be attributed to impurities or variations in its properties caused by the extrusion process. The surface is rough and irregular. The ribbed structure may result from the movement of the printhead during the extrusion and cooling process, and it may be also affected by heat retention in the sample.

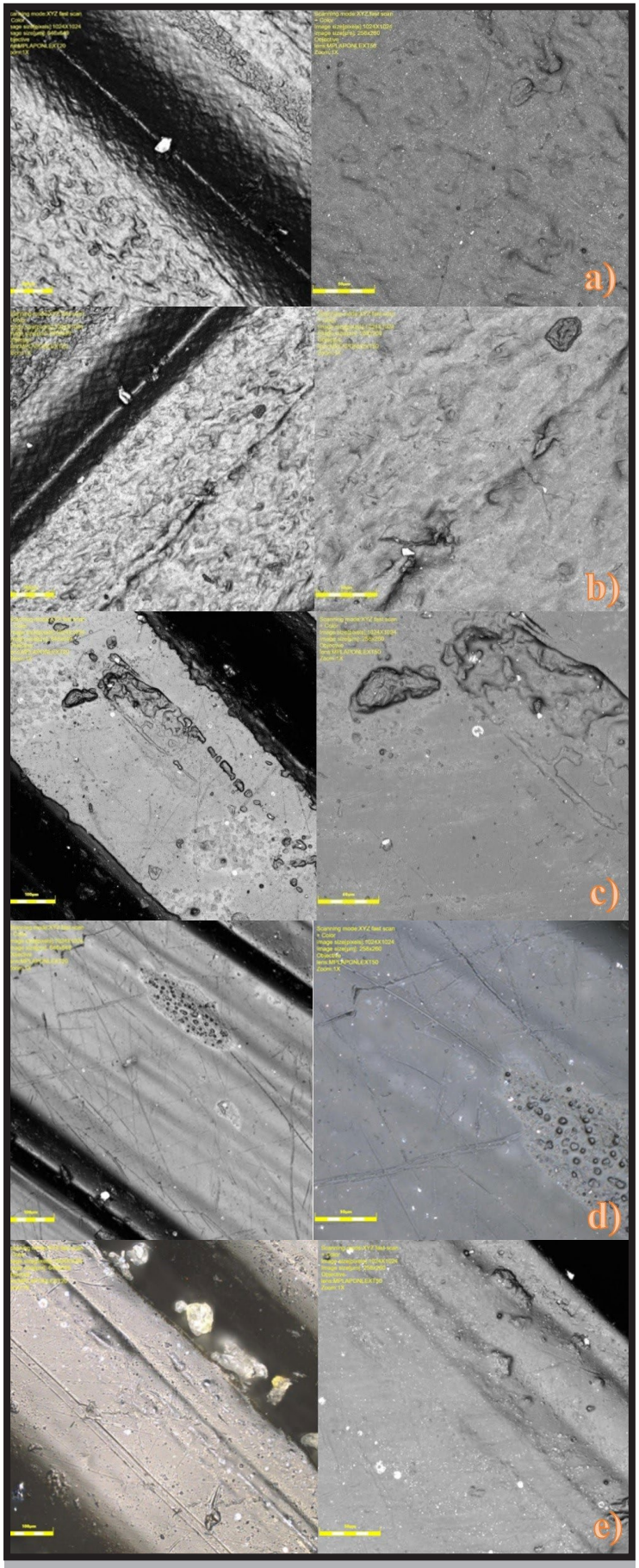

FIG. 6. Confocal microscope images of a reference sample of PLA material after tribological testing immersed in: a) Cl_2, b) H_2O in relation to PLA material with the addition of basalt immersed in: c) Cl_2, d) H_2O, e) swimming pool water.

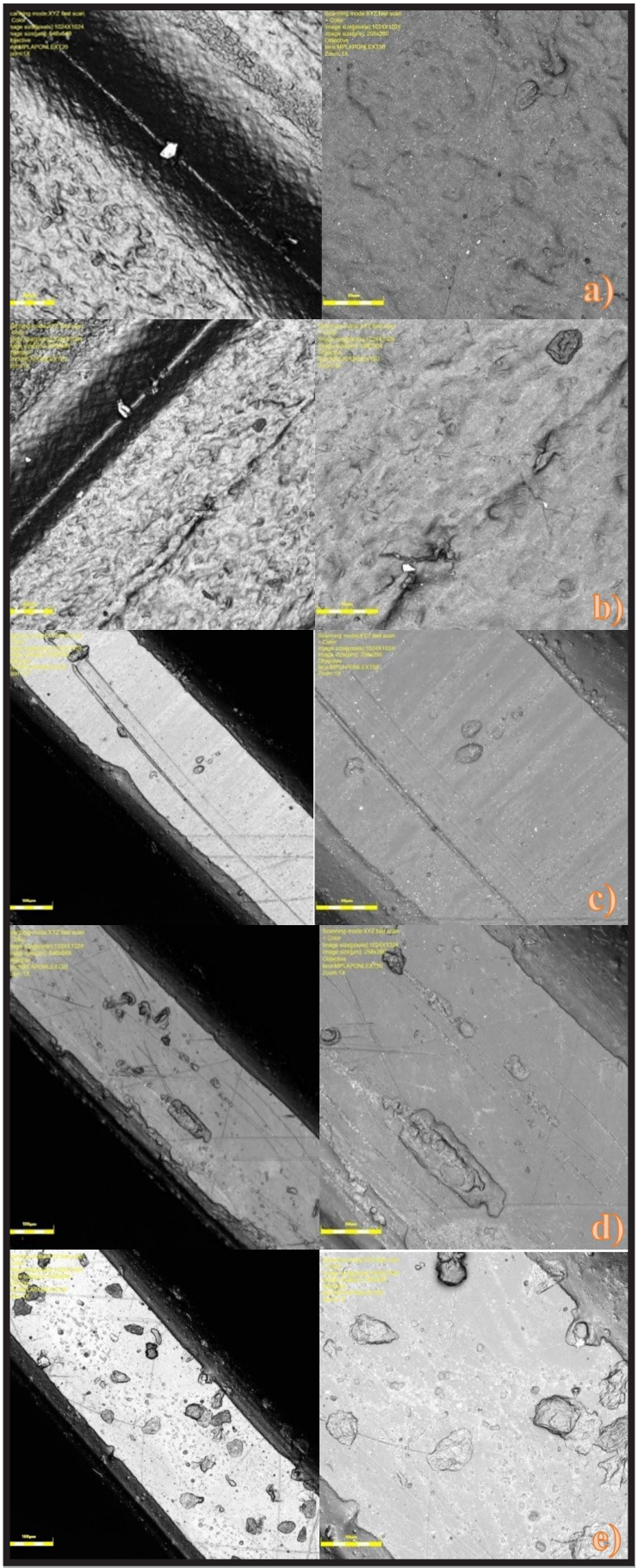

FIG. 7. Confocal microscope images of a reference sample of PLA material after tribological testing immersed in: a) Cl_2, b) H_2O in relation to PLA material with the addition of SiO_2 immersed in: c) Cl_2, d) H_2O, e) swimming pool water.

Additionally, the PLA surface morphology can be impacted by processing conditions, such as temperature, cooling rate, and pressure. The PLA material is hydrophilic, so it can easily absorb moisture from the environment, including water. Being soaked in H_2O, PLA can swell and soften, which leads to a decrease in its mechanical strength and stiffness [17,18]. The degree of swelling and changes in the PLA properties depend on the duration, temperature, and pH of the water. Soaking the samples for 7 days did not cause significant changes in the morphological structure of the material. On the contrary, wetting PLA in a chlorine solution can lead to its dissolution and degradation. Chlorine is a strong oxidant and can react with ester groups in the PLA polymer chains, which leads to acid hydrolysate and polymer decomposition [16,19].

The result of wetting PLA in chlorine dilution depends on the duration and concentration of the solution. In the images from the confocal microscope (FIGs 6b and 7b), one can observe the surface morphology after 7 days of soaking the material in free chlorine. The surface roughness increased. The shape was more irregular and the structure was rougher. It proves that chlorine affects the morphological properties of PLA, thus changing its mechanical properties. In turn, the PLA behavior in pool water shows its susceptibility to hydrolysis, which is a chemical reaction that occurs when water molecules break down the polymer chains in the material. This can reduce the material mechanical strength and other physical properties over time [20]. However, if the PLA material is properly reinforced and protected from the effects of H_2O and chlorine solution, it can retain its strength and shape. The PLA enriched with modifiers such as basalt and SiO_2 increases its resistance to various environments.

Analyzing the above confocal microscope images, it can be seen that the surface of PLA with the addition of basalt (FIGs 6c, d, e) is rougher than the surface with SiO_2 (FIGs 7c, d, e). The reason lies in the nature of basalt, as it is a volcanic mineral with a rougher surface than silica [6]. These differences can affect surface properties, such as adhesion and wettability. The addition of SiO_2 also supports a regular distribution of grains on the PLA surface, which can affect mechanical properties, such as stiffness and tensile strength. In the presence of basalt, there is a more random distribution of grains on the surface, which affects the mechanical properties. The addition of SiO_2 or basalt may influence the PLA structure. In the presence of silica (FIGs 7c, d, e), a more even and regular fibers distribution is visible in the entire structure of the PLA material. On the other hand, the basalt addition results in an irregular structure with protrusions of irregular shapes (FIGs 6c,d,e).

The study using the ball-disk friction node on the Anton-Paar device (Tribometer - TRN, Corcelles-Cormondrèche, Switzerland) and a profilographometer provided information on the mechanical properties of PLA, PLA/basalt and PLA/SiO_2 samples. This study also assessed the properties changes after the samples were immersed in pool water, chlorine solution, and distilled water for 7 days. The parameters such as: average coefficient of friction (FIG. 8), average area of the wear trace (FIG. 9) and volumetric wear (FIG. 10) were determined. The results are presented in the form of graphs.

FIG. 8 shows the average coefficient of friction for the tested samples. The higher the friction coefficient, the greater the friction force that occurs between the two surfaces [21]. Based on the given graph, it is possible to compare the resistance of each sample and identify the samples with greater resistance to friction. The PLA_Cl_2 sample has the lowest average friction coefficient ($\mu = 0.301$), which proves its higher resistance to friction as compared to the other samples. On the other hand, the PLA_H_2O sample has a higher average friction coefficient ($\mu = 0.443$), which suggests its lower friction resistance compared to the PLA_Cl_2 sample. The highest average coefficient of friction is 0.486 for the PLA_SiO_2_Cl_2 sample. Thus, this sample is the least resistant to wear in contact with chlorinated substances, compared to the other samples containing an admixture of SiO_2 or basalt. FIG. 9 represents the Area Wear Track obtained during the tribological test. The values differ significantly between individual samples, which means that the presence of the modifier and immersion of the material in the solutions had a significant impact on their wear.

The smaller the average area of the wear trace, the greater the wear resistance and durability of the material [21]. It can also be concluded that PLA in contact with water has the highest average wear trace area (714750 μm^2), so this material is the least resistant to abrasion compared to the other tested samples. The PLA_basalt_H_2O sample has a lower value (126500 μm^2) than the PLA_SiO_2_H_2O one with the average of 132250 μm^2, which proves its better wear resistance. Among the samples in contact with chlorine, the PLA_basalt_Cl_2 one revealed the highest average surface of the wear trace (474,750 μm^2). The PLA_SiO_2_Cl_2 obtained the lower wear surface value (113925 μm^2) than PLA_Cl_2 (169000 μm^2). It can be concluded that the PLA_basalt_Cl_2 is the least resistant to abrasion in contact with chlorine chemicals. Summing up, as compared to basalt, SiO_2 is a better modifier of PLA matrix in terms of abrasion resistance, in the presence of chlorine, water, or pool water which usually reduce this resistance. Analyzing the volumetric wear results in FIG. 10, the smallest wear occurred in the PLA_basalt_H_2O ($2.531 \cdot 10^{-3}$ mm^3/Nm) sample, i.e. during the water test. On the other hand, a higher consumption was observed in the PLA_H_2O sample ($1.43 \cdot 10^{-2}$ mm^3/Nm) but this value was several times higher than in the other samples. Comparing the results for each sample, the presence of chlorine in the environment reduced the volume consumption in the samples" PLA_basalt_Cl_2 ($9.498 \cdot 10^{-3}$ mm^3/Nm), PLA_SiO_2_Cl_2 ($2.279 \cdot 10^{-3}$ mm^3/Nm) and PLA_Cl_2 ($3.381 \cdot 10^{-3}$ mm^3/Nm), as compared to the samples without chlorine. However, in the PLA_basalt_pool sample, the presence of pool water significantly increased the volume consumption ($1.324 \cdot 10^{-2}$ mm^3/Nm), compared to the PLA_SiO_2_pool sample ($2.511 \cdot 10^{-3}$ mm^3/Nm). It is also worth mentioning that the smallest standard deviation (the smallest variability of the results) was revealed by the PLA_basalt_H_2O sample ($7.026 \cdot 10^{-5}$ mm^3/Nm).

The micromechanical tests using the Micro Combi Tester MCT3 device, determined the hardness and elasticity modulus of the samples - parameters important when choosing the right materials for medical applications and 3D printing. Thanks to the indentation (cavities), the load-unload curves (FIGs 11 and 12) were recorded for each sample to obtain information about the hardness and other mechanical properties. The following parameters were calculated: the Young's instrumental modulus, instrumental hardness, work of elastic and plastic deformation, total indentation work, maximum indentation depth, and elastic component of indentation work.

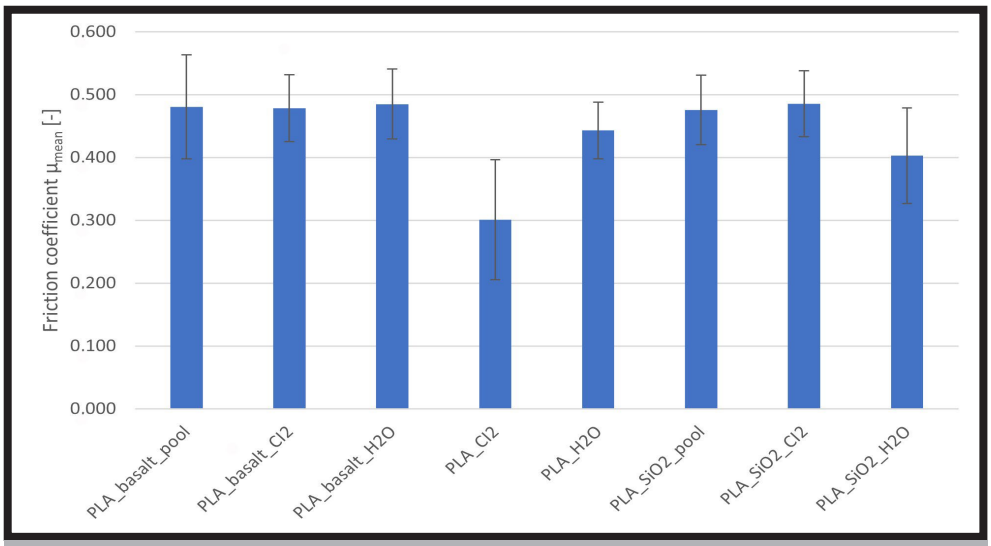

FIG. 8. Average friction coefficient.

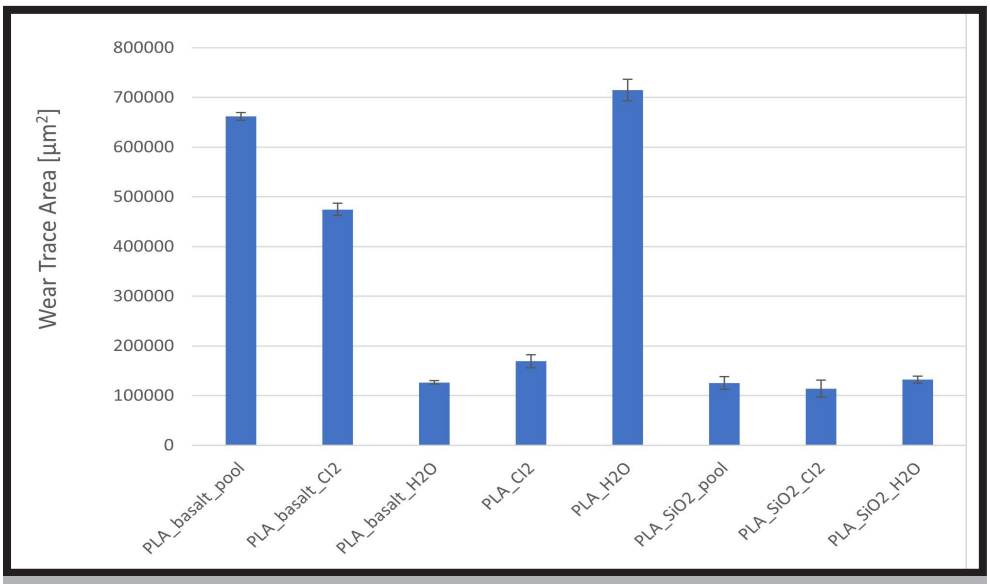

FIG. 9. Average wear trace area.

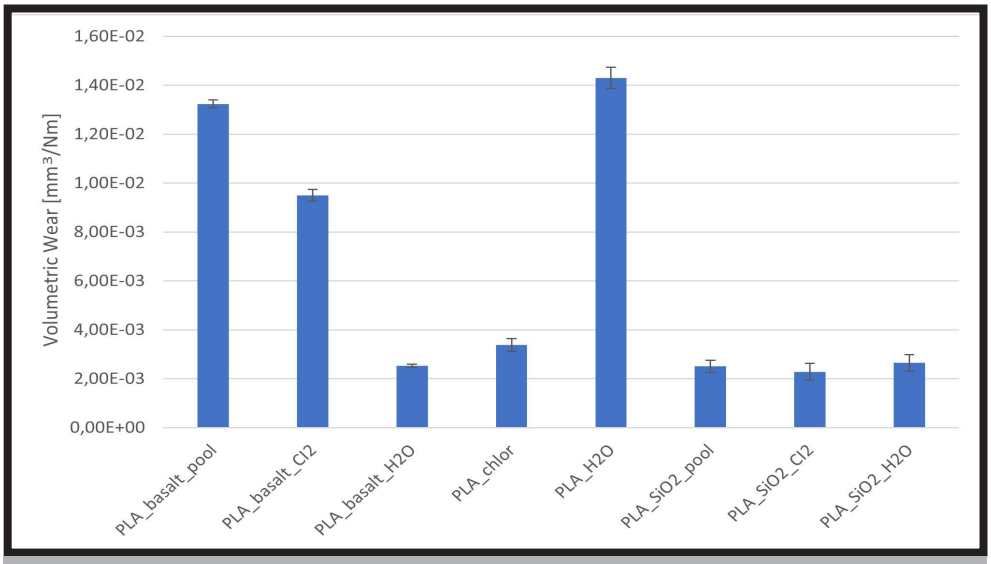

FIG. 10. Volumetric wear.

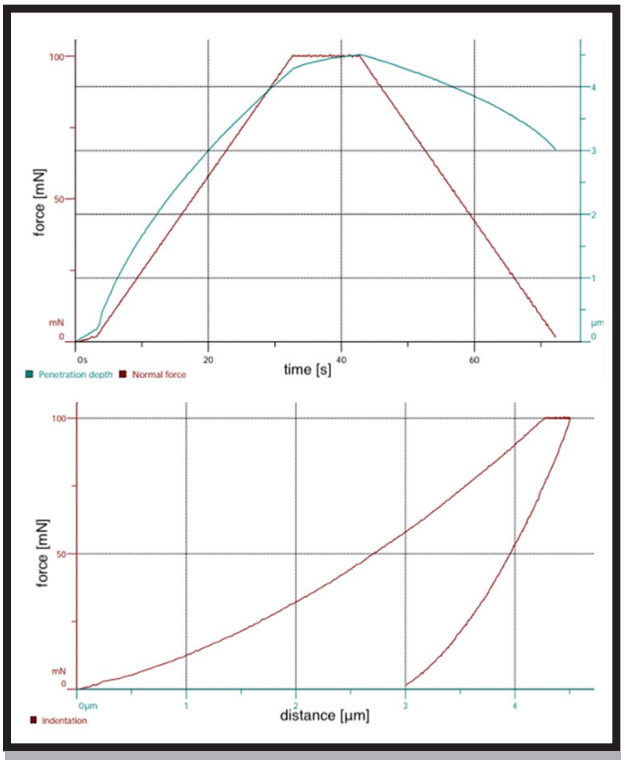

FIG. 11. Example of load-unload curves after indentation for PLA_SiO_2_pool samples.

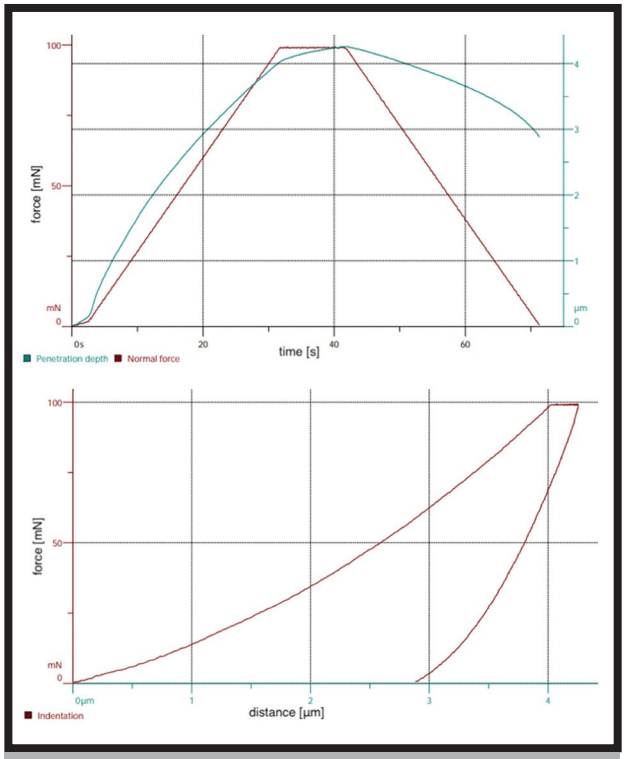

FIG. 12. Example of load-unload curves after indentation for PLA_basalt_Cl_2 samples.

TABLE 1. Results of micromechanical test samples, E_{IT} - indentation modulus of elasticity, H_{IT} – hardness, W_{el} – elastic forces, W_{pl} - plastic forces, W_{tot} – total forces, Hmax - maximum indentation depth, η_{IT} - elastic component of indentation work.

Name	E_{IT} [GPa]	H_{IT} [MPa]	W_{el} [MJ]	W_{pl} [MJ]	W_{tot} [MJ]	Hmax [Mm]	η_{IT} [%]
PLA_BASALT_POOL	5.488	0.323	0.051	0.127	0.177	4.067	28.652
	0.114	0.008	0.002	0.004	0.006	0.029	0.424
PLA_BASALT_Cl_2	5.366	0.293	0.052	0.13	0.181	4.254	28.51
	0.078	0.003	0.001	0.001	0.001	0.018	0.495
PLA_BASALT_H_2O	3.192	0.249	0.075	0.135	0.209	4.911	35.594
	0.059	0.009	0.002	0.002	0.004	0.057	0.315
PLA_Cl_2	5.661	0.310	0.049	0.131	0.18	4.099	27.608
	0.11	0.022	0.003	0.018	0.015	0.047	3.788
PLA_H_2O	5.918	0.336	0.051	0.117	0.168	4.02	30.394
	0.498	0.035	0.002	0.011	0.012	0.159	1.761
PLA_SiO_2_POOL	4.23	0.27	0.061	0.133	0.194	4.535	31.436
	0.1	0.005	0.002	0.001	0.003	0.03	0.481
PLA_SiO_2_Cl_2	3.885	0.264	0.065	0.134	0.199	4.636	32.603
	0.116	0.006	0.001	0.003	0.003	0.048	0.735
PLA_SiO_2_H_2O	3.079	0.247	0.075	0.139	0.214	4.94	35.144
	0.11	0.015	0.001	0.002	0.004	0.1	0.107

TABLE 1 presents results of the indentation modulus of elasticity (E_{IT}) for the tested samples. The E_{IT} values indicate the material stiffness, i.e. its ability to resist deformation. The higher the E_{IT} value, the stiffer the material. The PLA_BASALT_pool and PLA_BASALT_CI_2 revealed the E_{IT} values of 5.488 and 5.366 GPa, respectively. Both results were quite similar, suggesting that the chlorine solution immersion did not significantly affect the E_{IT} value. Therefore, basalt as a modifier in the material proved to be relatively stiff. The PLA_CI_2 samples immersed in chlorine solution and the PLA_H_2O samples in distilled water revealed their E_{IT} values to be 5.661 and 5.918 GPa, respectively. Both results were quite high, suggesting that the presence of chlorine and water positively effect the material stiffness. The PLA_SiO_2_pool, PLA_SiO_2_CI_2 and PLA_SiO_2_H_2O containing silica had the E_{IT} values amounting to 4.23, 3.885 and 3.079 GPa, respectively. Compared to the results for basalt and chlorine, these values were lower, indicating that silica is less rigid than basalt. The highest instrumental hardness value was obtained for the PLA_H_2O sample, and the lowest for PLA_SiO_2_H_2O. It is worth noting that the samples immersed in chlorine dilution (PLA_basalt_CI_2 and PLA_SiO_2_CI_2) had lower hardness than the samples immersed in pool water (PLA_basalt_pool and PLA_SiO_2_pool). Similarly, the PLA_basalt_H_2O sample had a lower hardness than the PLA_basalt_pool sample after immersion in the respective environment. Analyzing the results, it can be seen that the samples containing additives (basalt, chlorine, SiO_2) showed H_{IT} values comparable to the samples without additives (PLA_H_2O, PLA_CI_2). In conclusion, the additives did not significantly affect the hardness of the PLA material.

The test results also showed the values of elastic forces (W_{el}), plastic forces (W_{pl}), and total forces (W_{tot}). Compared to the reference samples (without modifiers), the PLA samples with basalt showed the higher elastic force, which means that the material was more resistant to deformation. At the same time, it was less plastic (lower plastic force). The samples after immersion in chlorine dilution and H_2O showed a lower value of elastic and plastic force than the control samples. The addition of SiO_2 lowered the elastic and total force, but the plastic force value was close to the one of the control samples. These results suggest that the basalt addition can improve the PLA mechanical strength but at the expense of its ductility, while the immersion in chlorine dilution and H_2O can weaken the mechanical strength. The SiO_2 addition can negatively affect the elastic and total strength, but it minimally influences the plastic strength.

Analyzing the results of the maximum indentation depth (Hmax), the PLA with basalt and the PLA with SiO_2 reached the highest Hmax (4.067 μm and 4.535 μm, respectively). This means that these additives in the material increased its resistance to deformation. The PLA samples after immersion in H_2O and chlorine dilution reached the lowest Hmax values (4.02 μm and 4.099 μm, respectively), so the additives reduced the resistance. The higher the Hmax value, the more resistant to deformation the material is. It can also be seen that the samples immersion in H_2O reduced the Hmax more than chlorine, which indicates the greater stiffness of the material in chlorine dilution. On the other hand, the addition of basalt and SiO_2 introduces elements with greater hardness into the material, which increases its resistance to deformation.

The results presented in the η_{IT} [%] column refer to the elastic component of indentation work. The η_{IT} value of all the samples was relatively high, which means that most of the indentation work was used for elastic deformation. The highest η_{IT} value of 35.594% was observed for the PLA_basalt_H_2O sample, so this material has the greatest ability to deform reversibly under pressing. The lowest η_{IT} value of 27.608% was revealed the PLA_CI_2 sample, which means its lower elastic deformation capacity.

The analysis showed that the both basalt and SiO_2 modifiers had an impact on the PLA mechanical properties. The addition of basalt slightly shifted the characteristic absorption bands associated with carbonyl ester groups and methyl groups in the FTIR analysis. In turn, SiO_2 affected the intensity and shape of the absorption bands. Basalt facilitated the material strength, which was manifested by a greater force required to break it. Basalt also improved the material elasticity, which manifested itself in greater resistance to deformation and cracking. In turn, the SiO_2 addition had a smaller effect on the elastic and plastic strength of the material. Based on the E_{IT} results for the tested samples, it can be concluded that basalt as a modifier in the material is relatively stiff. This was proved by the similar E_{IT} results for the samples immersed in pool water and chlorine. The lower E_{IT} scores for the silica samples revealed them to be less stiff than the basalt ones, as the higher the E_{IT}, the stiffer the material. The basalt samples showed the higher instrumental hardness than the samples without the modifier. They also showed a higher elastic force (W_{el}), which means they are more resistant to deformation, but at the same time they are less plastic (lower plastic force – W_{pl}). In contrast, the silica samples had the lower E_{IT} values than the basalt ones, thus, silica is less rigid than basalt. The silica sample showed the lowest instrumental hardness, proving its lower resistance to deformation than the other samples. The E_{IT} values for the samples with basalt were quite similar, so the immersion in chlorine solution had no significant effect on their stiffness. The basalt materials showed the high instrumental hardness, proving their resistance to deformation. The elastic forces (W_{el}) for the basalt samples were higher, indicating their greater resistance to deformation. Yet, the plastic forces (W_{pl}) were lower, which means the lower plasticity. The silica samples showed the lower instrumental hardness, which means the lower resistance to deformation compared to the basalt samples. In conclusion, in terms of the corrosive environment, the basalt-enhanced materials showed similar stiffness values, regardless of the immersion in different solutions. These materials are relatively stiff and deformation resistant, but less ductile. On the other hand, the silica-enhanced materials are less stiff and less resistant to deformation. Unfortunately, it is not possible to supplement the research results with the mechanical properties of the pure PLA and the PLA doped in the initial state, as these are topics for further research.

Conclusions

The study aimed to investigate the effects of modifiers, such as basalt and SiO_2, on the properties of the PLA composite material. The material was obtained through extrusion and 3D printing, and its chemical composition was analyzed using the FTIR spectroscopy. The immersion tests in different solutions revealed that the characteristic absorption bands of the material remained unchanged. The confocal microscopy provided the information on the surface structure of the tested samples. The immersion in water, chlorine, and pool water affected the material mechanical strength and physical properties, due to swelling, dissolution, and hydrolysis. The presence of modifiers influenced the morphological structure. The tribological tests demonstrated that the wear characteristics varied significantly between the samples, hence the modifiers and the solution immersion affected their wear and durability. Basalt enhanced the abrasion resistance, especially in the presence of chlorine, while silica had a positive effect on stiffness. Chlorine and water increased the material stiffness but the modifiers did not significantly affect hardness. The basalt-modified samples showed the higher elastic force and resistance to deformation but lower plasticity. Overall, the modifiers positively influenced the PLA properties, proving a potential for modifying its mechanical strength, chemical resistance, and plasticity. The research findings contributed to improving the 3D printing technology and enhancing the product quality. The results led to the better understanding of the material behavior at a microscopic level, particularly for advanced materials used in water and medical rescue applications.

Acknowledgments

The work was carried out as part of the statutory research of the Institute of Biomedical Engineering.

ORCID iD

M. Pyza: https://orcid.org/0000-0002-7904-9303
N. Brzezińska: https://orcid.org/0000-0002-8648-2498
K. Kulińska: https://orcid.org/0000-0002-6676-1502
J. Gabor: https://orcid.org/0000-0003-4850-1608
A. Barylski: https://orcid.org/0000-0002-1863-1471
K. Aniołek: https://orcid.org/0000-0002-5382-2038
Ż. Garczyk-Mundała: https://orcid.org/0000-0003-4345-5315
K. Adebesin: https://orcid.org/0000-0003-1841-0588
A. Swinarew: https://orcid.org/0000-0001-6116-9510

References

[1] W. Kanabenja, K. Passarapark: 3D printing filaments from plasticized Polyhydroxybutyrate/Polylactic acid blends reinforced with hydroxyapatite. Additive Manufacturing (2022). https://doi.org/10.1016/j.addma.2022.103130
[2] V. Nagarajan, A.K. Mohanty, M. Misra: Perspective on Polylactic Acid (PLA) based Sustainable Materials for Durable Applications: Focus on Toughness and Heat Resistance. ACS Sustainable Chemistry & Engineering 4(6) (2016) 2899-2916. https://doi.org/10.1021/acssuschemeng.6b00321
[3] B. Bax, J. Müssig: Impact and tensile properties of PLA/Cordenka and PLA/flax composites. Composites Science and Technology 68 (2008) 1601-1607.
https://doi.org/10.1016/j.compscitech.2008.01.004
[4] S. Łabużek, B. Nowak, J. Pająk, G. Rymarz: Activity of extracellular depolymerase secreted by Gliocladium solani strain during "Bionolle®" polyester degradation. Polimery 53 (2008) 465-470.
[5] P. Ruśkowski, A. Gadomska-Gajadhur: Polilaktyd w zastosowaniach medycznych: Tworzywa Sztuczne w Przemyśle 2 (2017) 32-35.
[6] V. Dhand, G. Mittal, K. Yop Rhee et al.: A short review on basalt fiber reinforced polymer composites, Composites Part B Engineering 73 (2015) 166-180.
[7] Yi Zhang, Junrong Yu, Chengjun Zhou et al.: Preparation, morphology, and adhesive and mechanical properties of ultrahigh-molecular-weight polyethylene/SiO_2 nanocomposite fibers. Polymer Composites 31(4) (2010) 684-690. https://doi.org/10.1002/pc.20847
[8] A. Ostrowski: Łódź wielofunkcyjna. Zgłoszony: 09.12.2013. Ochronny wzór użytkowy PL 67456.
[9] H. Czichos, S. Becker, J. Lexow: Multilaboratory tribotesting: results from the VAMAS program on wear test methods. Wear 114 (1987) 109-130.
[10] ASTM Standard G133-05, Standard Test Method for Linearly Reciprocating Ball-on-Flat Sliding Wear, ASTM International, West Conshohocken, PA (2016).
[11] W.C. Oliver, G.M. Pharr: An improved technique for determining hardness and elastic modulus using load and displacement sensing indentation experiments. J. of Mater. Res. 7 (1992) 1564-1583. https://doi.org/10.1557/JMR.1992.1564;
[12] ISO 14577-4, Metallic materials - Instrumented indentation test for hardness and materials parameters - Part 4: Test method for metallic and non-metallic coatings (2016).
[13] G. Mele, E. Bloise, F. Cosentino et al.: Influence of Cardanol Oil on the Properties of Poly(lactic acid) Films Produced by Melt Extrusion. ACS Omega 4(1) (2019) 718-726.
DOI: 10.1021/acsomega.8b02880
[14] https://www.sciencedirect.com/science/article/abs/pii/S0142941811001899?via%3Dihub
[15] B. Wei, S. Song, H. Cao: Strengthening of basalt fibers with nano-SiO_2–epoxy composite coating. Materials & Design 32(8-9) (2011) 4180-4186.
doi: https://doi.org/10.1016/j.matdes.2011.04.041
[16] G.H. Yew, A.M. Mohd Yusof, Z.A. Mohd Ishak et al.: Water absorption and enzymatic degradation of poly(lactic acid)/rice starch composites. Polymer Degradation and Stability 90(3) (2005) 488-500. https://doi.org/10.1016/j.polymdegradstab.2005.04.006
[17] G.L. Siparsky, K.J. Voorhees, J.R. Dorgan et al.: Water transport in polylactic acid (PLA), PLA/ polycaprolactone copolymers, and PLA/polyethylene glycol blends. J Environ Polym Degr 5 (1997) 125-136. https://doi.org/10.1007/BF02763656G
[18] F. Iñiguez-Franco, R. Auras, G. Burgess et al.: Concurrent solvent induced crystallization and hydrolytic degradation of PLA by water-ethanol solutions. Polymer 99 (2016) 315-323.
https://doi.org/10.1016/j.polymer.2016.07.018
[19] J.C. Fleischer, J.C. Diehl, L.S.G.L. Wauben et al.: The Effect of Chemical Cleaning on Mechanical Properties of Three-Dimensional Printed Polylactic Acid. J. Med. Device 14(1) (2020) 011109.
doi: 10.1115/1.4046120
[20] S.R. Subramaniam, M. Samykano, S.K. Selvamani, et al.: Preliminary investigations of polylactic acid (PLA) properties. AIP Conference 2059(1) (2019) 020038.
https://doi.org/10.1063/1.5085981
[21] M.M. Hanon, M. Kovács, L. Zsidai: Tribology behaviour investigation of 3D printed polymers, International Review of Applied Sciences and Engineering 10(2) (2019) 173-181.
https://doi.org/10.1556/1848.2019.0021